EurJIC
European Journal of Inorganic Chemistry

Research Article
doi.org/10.1002/ejic.202400080

Chemistry Europe
European Chemical Societies Publishing

www.eurjic.org

# Substituted Pyrrole-based Schiff Bases: Effect On The Luminescence Of Neutral Heteroleptic Cu(I) Complexes

Valentina Ferraro,*[a] Olaf Fuhr,[b] Claudia Bizzarri,[a] and Stefan Bräse*[a, c]

Neutral Cu(I) complexes containing Schiff bases as chelating N-donors and phosphines as P-donors were efficiently isolated and characterized. The imines were obtained by straightforward condensation between pyrrole-2-carboxaldehyde and the corresponding aromatic amines. The structure of most of the Cu(I) species was elucidated through single-crystal X-ray diffraction. The Cu(I) complexes exhibited intense absorptions around 400–500 nm ascribed to MLCT transitions. For some Cu(I) derivatives, orange- and red-orange emissions were detected upon excitation with near-UV and blue irradiation in the solid state. The emission maxima were red-shifted once the benzothiazole-derived Schiff base or Xantphos were employed as chelating ligands. Microsecond-long lifetimes, wide emissions, and large Stokes shifts suggest the involvement of triplet states in the luminescent process. Electrochemical measurements and DFT calculations were employed to rationalize the photoluminescence properties, which were ascribed to mixed $^3$LC/$^3$MLCT transitions.

## Introduction

Luminescent Cu(I) complexes have emerged as promising alternatives to second- and third-transition metals, such as Pt(II) and Ir(III), for a wide variety of applications.[1–5] Cu(I) derivatives have successfully been applied in organic light-emitting diodes (OLEDs),[6] light-emitting electrochemical cells (LECs),[7] solar cells[8] as well as photocatalysis.[9–13] Earth-abundant metals, such as Cu, are less expensive and toxic compared to precious elements such as Ru, Ir, Pt or Os.[3,14–15]

In most cases, the emission of Cu(I) complexes is ascribed to a metal-to-ligand charge transfer process involving triplet emitting states ($^3$MLCT). At the excited state, the metal is formally oxidized, whereas the ligands are reduced. Since the latter are directly involved in the emissive mechanism, minor modifications on their skeleton can cause noticeable differences in the photoluminescent properties. The majority of the heteroleptic Cu(I) complexes described in the literature are cationic compounds having a chelating N-donor ligand, and mono- or bidentate phosphines. In this case, the highest occupied molecular orbital (HOMO) is primarily localized on the Cu(I) center and the P-donor ligand, while the lowest unoccupied molecular orbital (LUMO) is localized on the π* orbitals of the diimine.[1,16] In the presence of suitable ligands, Cu(I) derivatives can exhibit thermally activated delayed fluorescence (TADF), a feature that is particularly appealing for OLED technology, as both singlet and triplet excitons can be harvested.[6,17–20]

Further, Schiff bases are useful organic compounds that can easily be synthesized starting from an amine and an aldehyde and are widely applied as mono- and polydentate ligands towards transition metal complexes such as Fe(II), Co(II), Ni(II), Pt(II), Pd(II) and Zn(II).[21–26] Hence, neutral Schiff bases were successfully employed for the preparation of photoactive cationic Cu(I) complexes.[27–29]

Given our interest in luminescent Cu(I) derivatives,[30–37] we deemed it interesting to investigate the effect of substituted pyrrole-based Schiff bases in the photophysical properties of the derived complexes. The use of imines as chelating N-donors for Cu(I) was previously described by Eisenberg's group.[38] However, the investigation focused on the different photophysical properties passing from pyrrole- to indole-derived Schiff bases. Herein, we report the synthesis and characterization of a series of neutral heteroleptic Cu(I) complexes with deprotonated Schiff bases as N-donors. The ligands were obtained by straightforward condensation in the presence of activated molecular sieve.[39] Triphenylphosphine, bis[(2-diphenylphosphino)phenyl] ether (DPEphos) and (9,9-dimethyl-9*H*-xanthene-4,5-diyl)bis(diphenylphosphine) (Xantphos) were employed as P-donors due to the combination of steric hindrance and extended π-conjugated systems that are known to reduce the undesirable pseudo-Jahn-Teller distortion in the excited state.[40]

[a] *Dr. V. Ferraro, Dr. C. Bizzarri, Prof. Dr. S. Bräse*
*Institute for Organic Chemistry (IOC)*
*Karlsruhe Institute of Technology (KIT)*
*Kaiserstrasse 12, 76131 Karlsruhe, Germany*
*E-mail: valentina.ferraro@kit.edu*
*stefan.braese@kit.edu*

[b] *Dr. O. Fuhr*
*Institute of Nanotechnology (INT) and Karlsruhe Nano Micro Facility (KNMFi)*
*Karlsruhe Institute of Technology (KIT)*
*Kaiserstrasse 12, 76131 Karlsruhe, Germany*

[c] *Prof. Dr. S. Bräse*
*Institute of Biological and Chemical Systems – Functional Molecular Systems (IBCS-FMS)*
*Karlsruhe Institute of Technology (KIT)*
*Kaiserstrasse 12, 76131 Karlsruhe, Germany*

Research Article
doi.org/10.1002/ejic.202400080



## Results and Discussion

### Synthesis and Characterization of the Complexes

The Schiff bases were prepared by condensation of 1*H*-pyrrole-2-carboxaldehyde with the corresponding aromatic amine in the presence of 4 Å activated molecular sieve (Taguchi's method).[37] In most cases, the product did not require any further purification and was isolated as a microcrystalline solid. The formation of the desired product was confirmed by the appearance of a singlet between 8.21 and 8.78 ppm in the $^{1}$H NMR spectra ascribable to the iminic CH. The corresponding carbon was detected at around 150 ppm in the $^{13}$C NMR spectra. As depicted in Scheme 1, the ligands were then deprotonated using $^{t}$BuOK, and the mixture was added to a solution of CuCl and the chosen phosphine ($PPh_3$, DPEphos or Xantphos) in dry dichloromethane (DCM). After removing KCl through filtration, the corresponding neutral heteroleptic Cu(I) complexes were isolated as dark yellow solids in yields up to 86 %. The products revealed to be air-stable and did not require to be stored under inert atmosphere.

The presence of both N- and P-donor ligands was confirmed by $^{1}$H, $^{13}$C and $^{31}$P{$^{1}$H} NMR spectra. The disappearance of the proton at low fields related to the pyrrole-NH is diagnostic for the formation of the neutral Cu(I) complexes. Further, the $^{31}$P signal related to the phosphine is often broadened owing to fluxional behavior in solution. In particular, in the case of [Cu($L^5$)(DPEphos)] and [Cu($L^5$)(Xantphos)], two $^{31}$P signals were observable, probably due to an equilibrium between two different Cu(I) complexes in solution, favored by the presence of the chelating P-donors.

The structure of most of the Cu(I) complexes was confirmed via X-ray diffraction. Suitable crystals were collected from the slow diffusion of DCM/pentane or DCM/diethyl ether solutions. The molecular structure of the complexes with the general formula [Cu($L^1$)(PP)] where PP is $(PPh_3)_2$, DPEphos or Xantphos is depicted in Figure 1. All crystal structures with the other Schiff bases are given in the Supporting Information (Figures S1–S3). Further, crystal data and structural refinement are collected in Tables S1, S3, S5 and S7 and selected bond lengths and angles are shown in Tables S2, S4, S6 and S8.

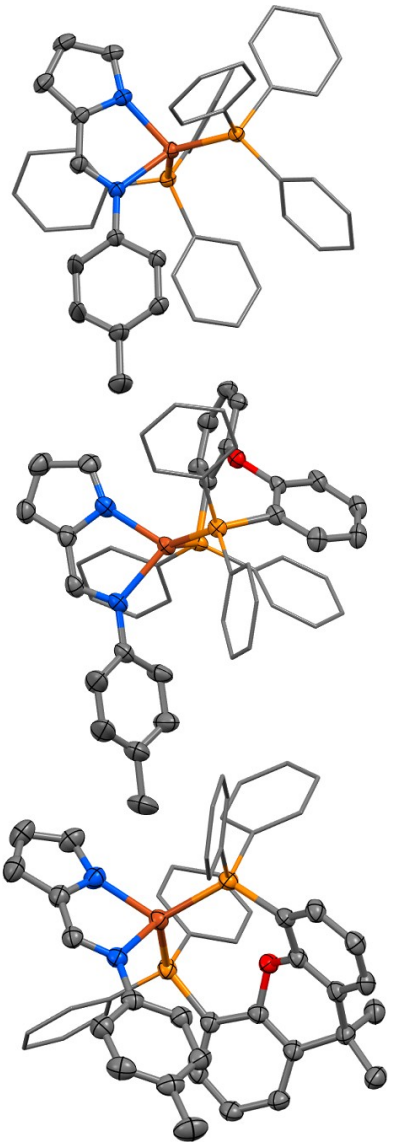

**Figure 1.** Molecular structure of [Cu($L^1$)(PP)] where PP is $(PPh_3)_2$, DPEphos or Xantphos (ellipsoid at 50 % probability level). Hydrogen atoms are omitted for clarity.

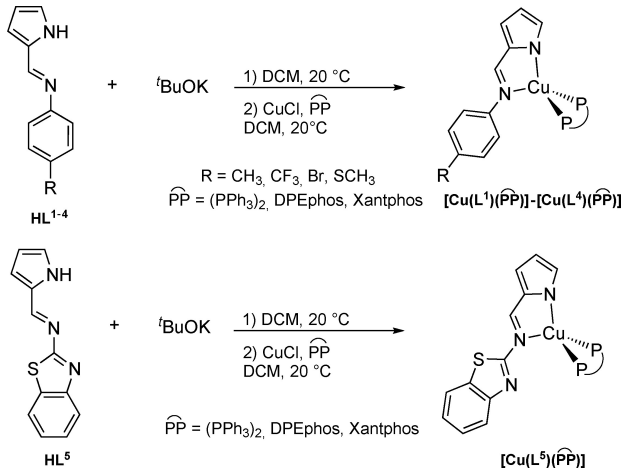


**Scheme 1.** Synthesis of the Cu(I) complexes.

The heteroleptic Cu(I) complexes crystallized either in the monoclinic (space group $P2_1/c$ or $P2_1/n$) or in the triclinic (space group $P\bar{1}$) system. The metal center is four-coordinated to two nitrogen and two phosphorus atoms in a distorted tetrahedral geometry. Similar to what was observed for analogous compounds,[38] the most irregular angle is N1-Cu1-N2 being around 80° for all the Cu(I) complexes. It is worth mentioning that the Cu(I) metal center in the molecular structure of [Cu($L^5$)(Xantphos)] is disordered in two positions. One is the proposed structure, while in the other one the ligand is coordinated to the metal center through the iminic nitrogen and the sulfur of the benzothiazole fragment.

Moreover, the phenyl fragment is inclined with respect to the plane containing the pyrrole ring and the imine group. This

Research Article
doi.org/10.1002/ejic.202400080


effect is more evident when DPEphos is used as P-donor ligand, probably due to π-π stacking interactions between the phosphine and the phenyl ring. In this case, the torsion angle is between 40° and 50°. On the other hand, the π-π stacking interaction and consequently the torsion is not observed with the benzothiazole moiety, and the ligand $L^5$ is almost planar in all the three Cu(I) derivatives [Cu($L^5$)(PP)] with PP = $(PPh_3)_2$, DPEphos or Xantphos.

### Electrochemical and Photoluminescent Properties

Cyclic voltammetry (CV) was conducted in dry DMF and under Argon atmosphere on all the luminescent Cu(I) complexes. The CV for [Cu($L^1$)$(PPh_3)_2$] and [Cu($L^5$)$(PPh_3)_2$] is depicted in Figure 2. Tetrabutylammonium hexafluorophosphate ($TBAPF_6$) and ferrocene were employed as supporting electrolyte and internal standard, respectively. Both Cu(I) complexes exhibit an irreversible peak around 0.5 V ascribable to the oxidation of the metal center to Cu(II). This is in line with previously described neutral Cu(I) complexes. Another oxidation process is observable around 0.8 V, probably due to the phosphines.[1]

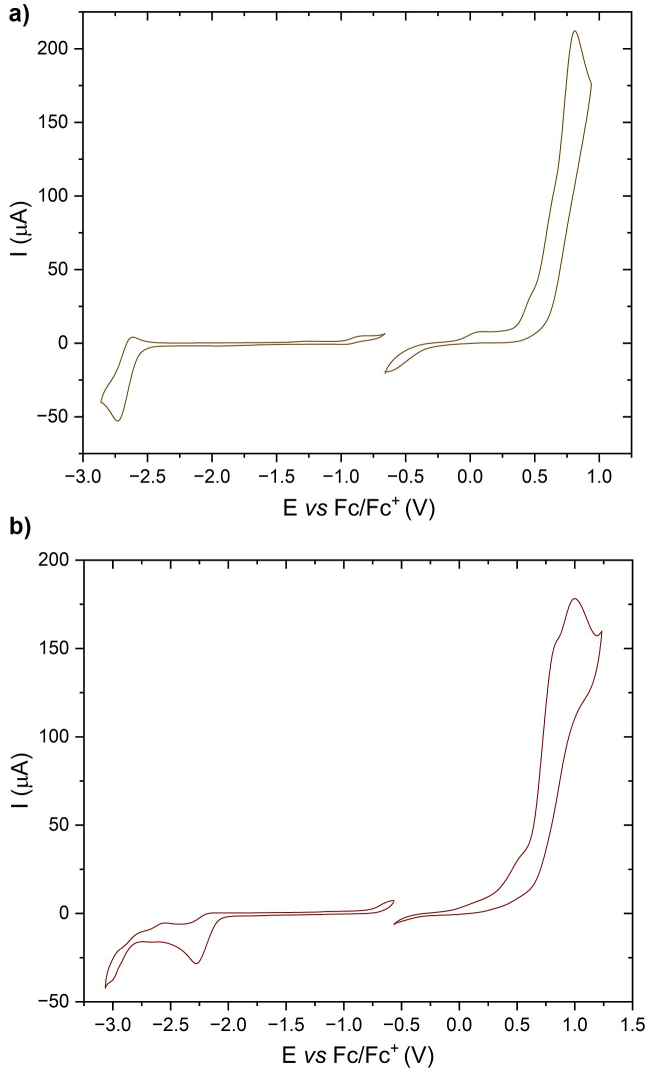


**Figure 2.** Cyclic voltammetry of [Cu($L^1$)$(PPh_3)_2$] (a) and [Cu($L^5$)$(PPh_3)_2$] (b) at 100 mV $s^{-1}$ in dry DMF ($5 \cdot 10^{-3}$ M) and Ar atmosphere (0.1 M $TBAPF_6$). Potentials are reported *vs.* ferrocene/ferrocenium ($Fc/Fc^+$) redox couple.

The peak in the reduction process is essentially attributable to the Schiff base ligand, as observable in the cationic wave of the corresponding free ligands $HL^1$ and $HL^5$ (see Figure S4). For [Cu($L^1$)$(PPh_3)_2$] the reduction peak is irreversible and lies at −2.73 V, while for $HL^1$ it is localized at −2.64 V. Instead, for [Cu($L^5$)$(PPh_3)_2$] the same peak is cathodically shifted at −2.28 V (−2.58 V for $HL^5$). An additional reduction peak is observed for the ligand $HL^5$ at −2.84 V. The potential gaps between the first oxidation and reduction peaks are respectively equal to 3.2 and 2.9 V and in line with the absorption spectra. The reduction and oxidation potentials of both Cu(I) complexes and ligands are summarized in Table S9. The cyclic voltammetries for all the [Cu(L)(PP)] with L = $L^1$, $L^2$, $L^3$ and $L^5$ and PP = $(PPh_3)_2$, DPEphos or Xantphos are depicted in Figures S5–S8 and the corresponding oxidation and reduction potentials are collected in Table S10. The possible discrepancies between the photoluminescent and the cyclovoltammetric data can be justified considering that they were collected in the solid state and in solution, respectively. Therefore, the interaction between the molecules and the possible formation of aggregates are not compensated by the solvent during the CV measurements and they are mostly disregarded.

The Cu(I) complexes were intensely colored both as powders and in concentrated solutions. The UV-vis spectra in DCM are characterized by absorptions below 500 nm. As observable in Table 1, the maximum molar coefficients are between 25200 and 58300 $M^{-1}cm^{-1}$. The band associated with the MLCT transition is observable between 400 and 500 nm. This band is shifted towards the blue region of the spectrum for the three [Cu($L^5$)(PP)] derivatives (PP = $(PPh_3)_2$, DPEphos or Xantphos). In addition, the absorption associated with the π* ←π transitions of the phosphine ligands can be observed for wavelengths below 350 nm. The UV-vis spectra of [Cu($L^1$)$(PPh_3)_2$] and [Cu($L^5$)$(PPh_3)_2$] are provided in the Supporting Information (see Figure S9).

DFT and TD-DFT calculations (MN15/def2-SVP) were conducted on [Cu($L^1$)$(PPh_3)_2$] and [Cu($L^5$)$(PPh_3)_2$] at the ground state considering DCM as C-PCM. The MLCT nature was confirmed being the HOMO-LUMO transition mostly responsible for the lowest energy absorptions (see Table S11 for the complete data set). The computed $\lambda_{abs}$ are roughly in line with the experimental outcomes, with the maximum predicted respectively at 346 and 393 nm (see Table 1 for the experimentally obtained photoluminescence data). In both cases, the hole and electron distribution associated with the absorption highlights the negligible involvement of the phosphines, as observable in Figure 3. As observed for other anionic N-donors,[1] the HOMO is localized partially on $L^1$ and $L^5$, and not on the phosphine, increasing the intra-ligand charge transfer (LC) character of the lowest energy band.

No appreciable luminescence was detected for the complexes in solution at room temperature probably due to vibrational quenching and pseudo-Jahn Teller distortion. Therefore, the photoluminescence measurements were carried out

Research Article
doi.org/10.1002/ejic.202400080

Chemistry Europe
European Chemical Societies Publishing



**Table 1.** Selected photoluminescence data for the Cu(I) complexes.

| | $\lambda_{abs}$ [a], nm ($\varepsilon/10^4$ $M^{-1}cm^{-1}$) | $\lambda_{em}$ [b,c], nm (n.i.)[d] | PLE[b,e], nm (n.i.)[d] | Stokes shift, $cm^{-1}$ | $\tau$[b,f], µs | $\Phi$[b,g], % |
|---|---|---|---|---|---|---|
| [Cu($L^1$)($PPh_3$)$_2$] | <450, 258 (4.60), 395 (2.73) | 575 (0.94), 625 (1), 662 (0.50) | <480, 443 (1) | 7900 | 334 | 7 |
| [Cu($L^1$)(DPEphos)] | <450, 288 (3.60), 386 (3.54) | 599 (0.99), 649 (1), 679 (0.66) | <480, 450 (1) | 9200 | 212 | 5 |
| [Cu($L^1$)(Xantphos)] | <460, 292 (2.52), 393 (2.00) | 597 (1), 652 (0.86), 712 (0.31) | <480, 450 (1) | 8700 | 18 | 2 |
| [Cu($L^2$)($PPh_3$)$_2$] | <460, 257 (3.57), 407 (2.54) | 572 (1), 618 (0.71), 654 (0.33) | <500, 455 (1) | 7100 | 288 | 28 |
| [Cu($L^2$)(DPEphos)] | <460, 276 (3.20), 405 (4.04) | 573 (1), 617 (0.81), 672 (0.42) | <500 | 7200 | 20 | 2 |
| [Cu($L^2$)(Xantphos)] | <450, 291 (7.06), 405 (4.53) | 586 (1), 637 (0.70), 680 (0.28) | <500, 460 (1) | 7500 | 65 | 4 |
| [Cu($L^3$)($PPh_3$)$_2$] | <460, 257 (5.90), 401 (3.23) | 576 (1), 624 (0.89), 680 (0.45) | <500 | 7500 | 486 | 17 |
| [Cu($L^3$)(DPEphos)] | <460, 300 (4.37), 411 (4.15) | 570 (0.50), 609 (1), 660 (0.77) | <490 | 6600 | 277 | 8 |
| [Cu($L^3$)(Xantphos)] | <460, 276 (4.53), 400 (5.83) | 603 (1), 655 (0.93), 700 (0.52) | <500 | 8400 | 85 | 2 |
| [Cu($L^4$)($PPh_3$)$_2$] | <480, 260 (2.65), 403 (2.09) | – | – | – | – | – |
| [Cu($L^4$)(DPEphos)] | <470, 278 (2.32), 399 (2.16) | – | – | – | – | – |
| [Cu($L^4$)(Xantphos)] | <470, 289 (3.70), 407 (1.98) | – | – | – | – | – |
| [Cu($L^5$)($PPh_3$)$_2$] | <500, 267 (2.69), 442 (2.74) | 599 (0.97), 656 (1), 719 (0.59) | <500, 485 (1) | 5900 | 18 | 1 |
| [Cu($L^5$)(DPEphos)] | <500, 279 (2.62), 439 (3.18), 452 (sh) | 605 (1), 659 (0.79) | <500 | 6250 | 4 | 0.25 |
| [Cu($L^5$)(Xantphos)] | <500, 287 (3.09), 441 (3.27), 453 (sh) | 622 (1), 668 (0.94) | <500 | 6500 | 3 | 0.16 |

[a] DCM solution, rt. [b] Solid sample, rt. [c] $\lambda_{excitation}$ = 350 nm. [d] n.i. = normalized intensity. [e] $\lambda_{emission}$ = 570–600 nm. [f] $\lambda_{excitation}$ = 350–370 nm; $\lambda_{emission}$ = 570–650 nm. [g] $\lambda_{excitation}$ = 400–450 nm.

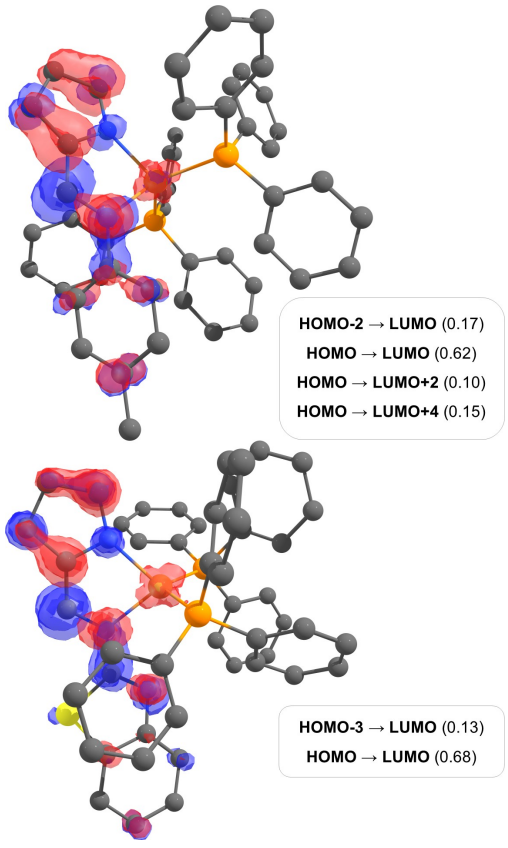


**Figure 3.** Hole (red) and electron (blue) distribution of ground singlet optimized structures for [Cu($L^1$)($PPh_3$)$_2$] and [Cu($L^5$)($PPh_3$)$_2$] related to the lowest energy singlet←singlet absorption (surface isovalue = 0.003 a.u.). Inset: orbitals involved in the absorption process together with the corresponding weighted coefficients in parenthesis. Color map: Cu, dark orange; S, yellow; P, orange; N, blue; C, grey. Hydrogen atoms are omitted for clarity.

on powder samples. Although the presence of a sulfur atom in the skeleton of the ligands was proven to enhance the photophysical features and the electric conductivity in the corresponding Cu(I) complexes,[41–44] the emissive properties of [Cu($L^4$)(PP)] were negligible also in the solid state, therefore they were not further investigated.

The Cu(I) complexes show orange to red-orange emission upon excitation with near UV and blue light. Normalized PL and PLE spectra for the representative [Cu($L^1$)($PPh_3$)$_2$] and [Cu($L^5$)($PPh_3$)$_2$] are provided in Figure 4. The Cu(I) complexes exhibit almost unitary color purity (see Figure S10 for the CIE 1931 chromaticity diagram). In all cases, the emission spectra are characterized by multiple peaks due to the vibronic structure, further supporting the mixed LC/MLCT nature of the emission.[45] The difference between the first and second vibronic bands is between 1300 and 1400 $cm^{-1}$. The difference is slightly lower for the second and third vibronic bands (1100–1200 $cm^{-1}$).

The emission maxima appear to be red-shifted when Xantphos was employed as P-donor or, more evidently, when $L^5$ was used as N-donor. The latter can be justified by considering the presence of a heavier atom in the skeleton of the ligand. Consequently, the photoluminescent lifetimes $\tau$ and quantum yields $\Phi$ are significantly lower for these Cu(I) complexes. This outcome can be partly justified considering the energy gap law, *i.e.* the increase of $k_{nr}$ due to vibrational coupling for longer wavelengths.[46–48] In contrast to what is commonly observed in similar Cu(I) complexes,[1,35,44] the use of chelating biphosphines such as DPEphos and Xantphos does not improve the photoluminescent features, presumably because the rigidification of the structure does not compensate the non-radiative processes. Moreover, it is widely recognized that a wide bite angle in the

Research Article
doi.org/10.1002/ejic.202400080


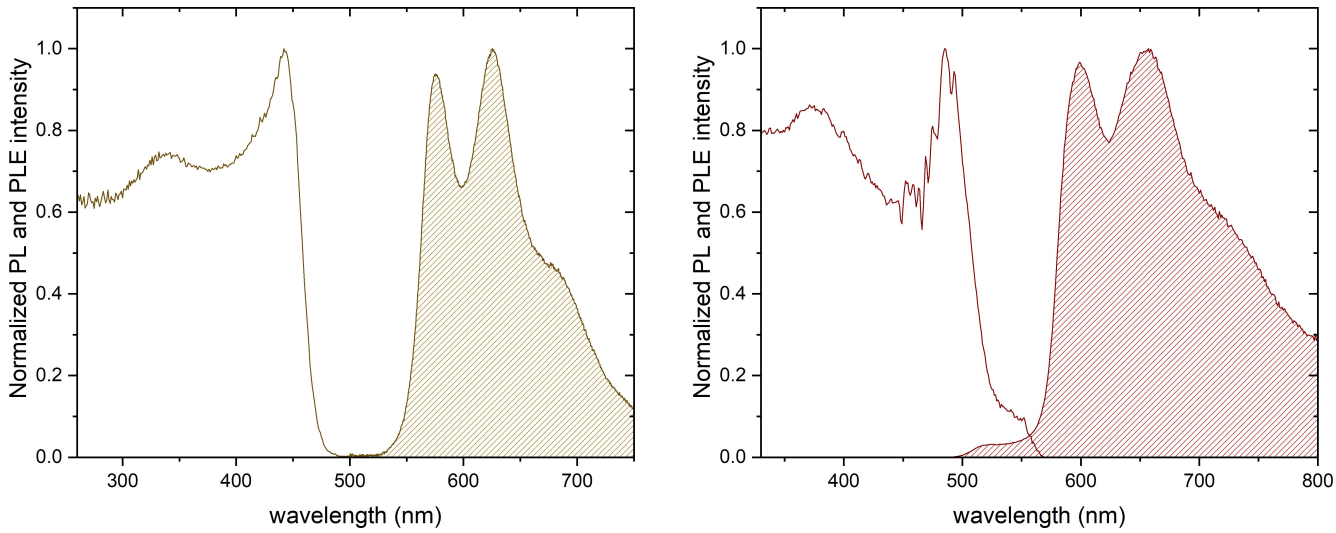


**Figure 4.** Normalized PL and PLE spectra of $[Cu(L^1)(PPh_3)_2]$ (on the left, $\lambda_{excitation} = 350$ nm, $\lambda_{emission} = 570$ nm) and $[Cu(L^5)(PPh_3)_2]$ (on the right, $\lambda_{excitation} = 450$ nm, $\lambda_{emission} = 600$ nm) collected in the solid state and at room temperature.

phosphines determined improved photophysical properties of the corresponding Cu(I) complexes.[48–51] In this case, $PPh_3$ exhibited a higher P2-Cu1-P1 angle compared to DPEphos and Xantphos, thus supporting the enhanced emissive features of the related Cu(I) derivatives based on the former with respect to the latter (see Tables S2, S4, S6 and S8).

The photoluminescent lifetimes τ are all in the microsecond range, suggesting the involvement of triplet states in the emission as highlighted in Figure S11 for $[Cu(L^1)(PPh_3)_2]$ and $[Cu(L^5)(PPh_3)_2]$. This hypothesis is supported by the wide emissions and the Stokes shift comprised between 6250 and 9200 $cm^{-1}$. The longest τ, equal to 486 μs, was detected for $[Cu(L^3)(PPh_3)_2]$ and, although a clear trend could not be observed, the measured τ is generally longer when $PPh_3$ is used as a P-donor. Similar considerations can be made for the Φ, and the highest value, equal to 28%, was measured for $[Cu(L^2)(PPh_3)_2]$. Remarkably, the higher HOMO-LUMO gap and the mixed LC/MLCT mechanism due to the presence of an anionic N-donor ligand determines an overall increase in the photoluminescent τ and Φ.[1,38] The emission and excitation spectra, as well as the photoluminescence lifetime decay curves for $[Cu(L^2)(PPh_3)_2]$ and $[Cu(L^3)(PPh_3)_2]$ are collected in Figures S12 and S13.

The emission mechanism of $[Cu(L^1)(PPh_3)_2]$ and $[Cu(L^5)(PPh_3)_2]$ was investigated through DFT and TD-DFT calculations considering the optimized triplet geometries. The structures are nearly superimposable with the corresponding singlet state, being the root-mean-square deviation (RMSD) of 0.798 and 0.079 Å for $[Cu(L^1)(PPh_3)_2]$ and $[Cu(L^5)(PPh_3)_2]$, respectively. The emission is predicted between 689 and 698 nm for both the Cu(I) derivatives, roughly in line with the experimental data (see Table 1). The emission is ascribed to a pure HOMO-LUMO transition for $[Cu(L^1)(PPh_3)_2]$, while in the case of $[Cu(L^5)(PPh_3)_2]$ also the HOMO-1 orbital is involved (see Table S11). Therefore, the hole-electron distribution is almost specular to the one observed for the corresponding singlet→singlet transition (see Figure S14 for the triplet→singlet transition). As previously observed for the absorption process, the phosphines are not involved in the emissive mechanism, thus the emission can be ascribed to a mixed $^3$LC/$^3$MLCT transition.

To conclude, based on TD-DFT calculations, the computed energy gaps between $^1$MLCT and $^3$MLCT do not support the possibility of a TADF mechanism since the ΔE is around 8000 $cm^{-1}$ (see Table S12), as TADF is only possible when the energy gap between the singlet and triplet MLCT is below 1500 $cm^{-1}$.[17]

## Conclusions

Heteroleptic neutral Cu(I) complexes having Schiff bases as chelating N-donor ligands were successfully synthesized and characterized. Appreciable orange-red luminescence was observed in the solid state with excitation in the near-UV and blue regions. The emission was ascribed to a mixed $^3$LC/$^3$MLCT based on experimental data and DFT calculations. The photophysical data highlights the dependence of photoluminescent lifetimes and quantum yields upon the choice of the P-donor ligand and the substituent on the *para*-position of the Schiff base. The longest τ was measured when $PPh_3$ and the bromo-substituted $HL^3$ were employed as P- and N-donor ligands, respectively. On the other hand, despite not being directly involved in the emission process, higher Φ were observed with triphenylphosphine regardless of the Schiff base used, owing to the wider bite angle compared to DPEphos and Xantphos. The emissive features were significantly lower when $L^5$ was coordinated to Cu(I), probably due to the bathochromic shift in the maxima and the consequent increase in the vibrational coupling.

To conclude, the photophysical properties of the here described Cu(I) complexes can be slightly tuned acting on the substituent in the *para*-position of the Schiff base. The intense absorption in the blue region makes these Cu(I) species suitable

Research Article
doi.org/10.1002/ejic.202400080





candidates to be applied in photocatalysis and the study presented here could help with the design of similar derivatives to be employed for such purpose.

## Experimental Section

### General Remarks

The solvents were purchased from Fisher, if not stated otherwise. Dichloromethane was dried with the solvent purification system (SPS) from MBraun (model MB-SPS-800) and was degassed with argon before usage for 5 min. The precipitation of the Cu(I) complexes was performed with *n*-pentane or diethyl ether purchased from Merck. CuCl was purchased from Merck together with potassium *tert*-butoxide ($^t$BuOK), triphenylphosphine, pyrrole-2-carboxaldehyde, *p*-toluidine, *p*-bromoaniline and 4-(methylthio)aniline. 4-(Trifluoromethyl)aniline and 2-aminobenzothiazole were acquired respectively from ChemPur and TCI Chemicals. DPEphos was obtained from Thermo Fisher, whereas Xantphos was from BLDPharm. All chemicals were used without any further purification. The heteronuclear NMR spectra of the Cu(I) complexes were recorded in $CDCl_3$ purchased from Eurisotop. All reactions were carried out using Schlenk techniques under Ar atmosphere.

General information concerning NMR, mass spectrometry, IR and elemental analyses, as well as melting points and single-crystal X-ray diffraction (XRD) analyses is detailed in the Supporting Information. Additional information on the experimental procedure is available via the Chemotion Repository.[52]

### Synthesis of the Ligands

The aromatic amine (4.67 mmol, 1.00 equiv) and 1*H*-pyrrole-2-carbaldehyde (444 mg, 4.67 mmol, 1.00 equiv) were added to a flask together with 5 g of activated molecular sieves 4 Å and 25 mL of dry DCM. In the case of (*E*)-*N*-(1,3-benzothiazol-2-yl)-1-(1*H*-pyrrol-2-yl)methanimine, dry toluene was used as solvent. The reaction mixture was refluxed for 24 hours, then the molecular sieves were filtered off, and the solvent was evaporated under reduced pressure. The product was treated with 5 mL of pentane to afford a solid that was filtered, washed with 2×2.5 mL of pentane, and dried *in vacuo*. In the case of (*E*)-*N*-(1,3-benzothiazol-2-yl)-1-(1*H*-pyrrol-2-yl)methanimine, the product was recrystallized from cold ethanol. The characterization data of $HL^1$, $HL^2$, $HL^3$ and $HL^5$ are in line with the one reported for the same compounds obtained with different experimental procedures.[53–56]

*Characterization of (E)-N-(4-(methylthio)phenyl)-1-(1H-pyrrol-2-yl)methanimine ($HL^4$).* $R_f = 0.62$ (*n*Hex/EtOAc 2:1). m.p.: 80 °C. $^1$H NMR (400 MHz, Chloroform-*d* [7.27 ppm], ppm) δ = 9.79 (br. s, 1H), 8.27 (s, 1H), 7.33–7.22 (m, 2H), 7.18–7.11 (m, 2H), 6.90–6.94 (m, 1H), 6.71–6.65 (m, 1H), 6.32–6.26 (m, 1H), 2.50 (s, 3H). $^{13}$C NMR (100 MHz, Chloroform-d [77.0 ppm], ppm) δ = 149.3, 135.3, 130.9, 128.1 (2C), 123.3, 121.6 (2C), 116.7, 111.5, 110.7, 16.7. MS (EI, 70 eV, 60 °C), m/z (%): 218.07 (5), 217.07 (16), 216.07 (100) $[M]^+$, 215.07 (72), 201.05 (27), 200.04 (12), 168.07 (19), 108.01 (5). HRMS-EI (m/z): $[M]^+$ calcd. for $C_{12}H_{12}N_2S$, 216.0716; found, 216.0717.

### Synthesis of the Complexes

The Schiff base (606 μmol, 1.20 equiv) was deprotonated using a stoichiometric amount of $^t$BuOK (68.0 mg, 606 μmol, 1.20 equiv) in 5 mL of dry DCM under Ar atmosphere. The reaction mixture was stirred for four hours, then transferred to a solution containing CuCl (50.0 mg, 505 μmol, 1.00 equiv) and PP (1.01 mmol, 2.00 equiv. for $PPh_3$; 505 μmol, 1.00 equiv. for DPEphos and Xantphos) in 3 mL of dry DCM. The solution rapidly changed to dark orange and KCl started to precipitate. The reaction mixture was stirred for 18 hours at 20 °C, then the salt was filtered off, and the solvent was evaporated under reduced pressure to afford an oil that was treated with 5 mL of pentane or diethyl ether. The product was filtered off, washed with 2×5 mL of pentane (or diethyl ether), and dried *in vacuo* to afford a dark yellow solid.

*Characterization of [Cu($L^1$)($PPh_3$)$_2$].* Yield: 64% (0.249 g). m.p. 140 °C. $^1$H NMR (400 MHz, Chloroform-*d* [7.27 ppm], ppm) δ = 8.21 (s, 1H, $L^1$), 7.28–7.18 (m, 6H, $PPh_3$), 7.16–7.06 (m, 24H, $PPh_3$), 7.00 (s, 1H, $L^1$), 6.86 (d, *J* = 3.4 Hz, 1H, $L^1$), 6.83–6.78 (m, 2H, $L^1$), 6.71–6.65 (m, 2H, $L^1$), 6.30 (dd, *J* = 1.3 Hz, *J* = 3.4 Hz, 1H, $L^1$), 2.23 (s, 3H, $L^1$). $^{31}$P{$^1$H} NMR (161 MHz, ppm) δ = −1.26. $^{13}$C NMR (100 MHz, Chloroform-*d* [77.0 ppm], ppm) δ = 153.4, 149.4, 140.7, 136.8, 134.8 (d, *J* = 22.2 Hz, 6C), 133.7 (d, *J* = 8.6 Hz, 12C), 133.1, 129.1 (2C), 129.0 (6C), 128.2 (d, *J* = 8.6 Hz, 12C), 121.6 (2C), 116.9, 111.5, 20.7. MS (FAB, 3-NBA), m/z (%):

678.04 (17), 676.04 (17), 590.11 (18), 589.11 (51) $[Cu(PPh_3)_2]^+$, 588.11 (41), 587.11 (100), 510.11 (10), 509.12 (15), 508.12 (10), 327.00 (29), 326.01 (13), 325.00 (62) $[Cu(PPh_3)]^+$, 307.08 (10) [3-NBA], 279.06 (13), 263.07 (10), 262.06 (15) $[PPh_3]$, 185.04 (23) [L], 184.05 (14), 183.00 (30), 155.03 (11), 154.02 (42) [3-NBA], 138.03 (14), 137.02 (25) [3-NBA], 136.01 (27), 107.02 (9), 88.99 (9). IR (ATR, $\tilde{\nu}$) = 3098 (vw), 3072 (w), 3054 (w), 3002 (w), 2985 (w), 2941 (w), 1562 (vs), 1509 (m), 1489 (w), 1477 (m), 1434 (s), 1408 (w), 1385 (m), 1341 (w), 1302 (vs), 1279 (m), 1266 (m), 1222 (w), 1186 (m), 1171 (m), 1156 (w), 1113 (w), 1094 (m), 1071 (w), 1037 (s), 997 (w), 977 (w), 955 (w), 932 (w), 891 (w), 880 (w), 827 (w), 813 (w), 795 (w), 742 (vs), 734 (vs), 691 (vs), 618 (w), 611 (w), 527 (w), 504 (vs), 490 (vs), 443 (w), 432 (w), 416 (w) $cm^{-1}$. EA ($C_{48}H_{41}CuN_2P_2$): Calcd C, 74.74; H, 5.36; N, 3.63. Found C, 73.68; H, 5.14; N, 3.74.

*Characterization of [Cu($L^1$)(DPEphos)].* Yield: 69% (0.275 g). m.p. 193 °C. $^1$H NMR (400 MHz, Chloroform-*d* [7.27 ppm], ppm) δ = 8.16 (s, 1H, $L^1$), 7.22–7.15 (m, 12H, DPEphos), 7.14–7.09 (m, 9H, DPEphos), 7.05 (s, 1H, $L^1$), 6.95–6.70 (m, 12H, $L^1$ + DPEphos), 6.25 (dd, *J* = 1.4 Hz, *J* = 3.4 Hz, 1H, $L^1$), 2.20 (s, 3H, $L^1$). $^{31}$P{$^1$H} NMR (161 MHz, ppm) δ = −15.02. $^{13}$C NMR (100 MHz, Chloroform-*d* [77.0 ppm], ppm) δ = 158.6 (t, *J* = 6.5 Hz, 2C), 152.7 (t, *J* = 2.9 Hz), 149.1 (2C), 140.6 (t, *J* = 1.5 Hz), 136.7, 134.3 (2C), 133.8 (t, *J* = 8.5 Hz, 6C), 133.0 (t, *J* = 14.8 Hz, 2C), 132.5 (2C), 130.5, 129.1 (2C), 129.0 (6C), 128.0 (t, *J* = 4.6 Hz, 8C), 126.5 (t, *J* = 11.5 Hz, 2C), 124.1 (2C), 121.5 (2C), 120.0 (2C), 116.1, 111.1, 20.7. MS (FAB, 3-NBA), m/z (%): 785.33 (6) $[M]^+$, 784.33 (5), 617.15 (6), 604.15 (19), 603.16 (51), 602.16 (41), 601.15 (100) $[Cu(DPEphos)]^+$, 353.14 (7), 307.11 (18) [3-NBA], 289.09 (7), 199.00 (12), 195.10 (6), 185.08 (6), 184.07 (6), 183.02 (12), 155.04 (18), 154.03 (61) [3-NBA], 152.04 (5), 139.05 (8), 138.05 (22), 137.04 (41) [3-NBA], 136.03 (41), 135.03 (5), 124.04 (5), 120.04 (6), 107.05 (13), 91.03 (8), 90.02 (7), 89.01 (12). IR (ATR, $\tilde{\nu}$) = 3068 (vw), 3050 (vw), 3030 (vw), 3021 (vw), 2963 (vw), 1562 (vs), 1508 (m), 1479 (w), 1461 (m), 1432 (vs), 1384 (s), 1337 (vw), 1295 (vs), 1281 (m), 1265 (w), 1257 (m), 1207 (vs), 1183 (s), 1171 (w), 1155 (w), 1128 (w), 1120 (w), 1108 (w), 1092 (m), 1069 (w), 1028 (vs), 997 (w), 977 (w), 958 (w), 950 (w), 936 (w), 919 (w), 893 (w), 882 (m), 871 (m), 854 (w), 828 (w), 819 (w), 799 (m), 764 (w), 745 (vs), 740 (vs), 732 (vs), 713 (w), 692 (vs), 668 (m), 643 (w), 614 (m), 585 (w), 544 (m), 532 (w), 522 (vs), 507 (vs), 492 (vs), 477 (vs), 465 (vs), 449 (m), 432 (s), 421 (s), 410 (vs) $cm^{-1}$. EA ($C_{48}H_{39}CuN_2OP_2$): Calcd C, 73.41; H, 5.01; N, 3.57. Found C, 73.00; H, 4.82; N, 3.63.

*Characterization of [Cu($L^1$)(Xantphos)].* Yield: 77% (0.323 g). m.p. 257 °C. $^1$H NMR (400 MHz, Chloroform-*d* [7.27 ppm], ppm) δ = 8.33 (s, 1H, $L^1$), 7.53 (dd, *J* = 1.5 Hz, *J* = 7.8 Hz, 2H, Xantphos), 7.20 (m, 8H,

Xantphos), 7.13–7.07 (m, 12H, Xantphos), 7.01 (t, $J$ = 7.7 Hz, 2H, Xantphos), 6.88 (d, $J$ = 3.5 Hz, 1H, $L^1$), 6.69–6.67 (m, 3H, $L^1$), 6.60 (d, $J$ = 8.1 Hz, 2H, Xantphos), 6.47–6.43 (m, 2H, Xantphos), 6.22 (dd, $J$ = 1.3 Hz, $J$ = 3.4 Hz, 1H, $L^1$), 2.15 (s, 3H, $L^1$), 1.80 (s, 3H, Xantphos), 1.71 (s, 3H, Xantphos). $^{31}P\{^1H\}$ NMR (161 MHz, ppm) δ = −14.17. $^{13}C$ NMR (100 MHz, Chloroform-*d* [77.0 ppm], ppm) δ = 155.4 (t, $J$ = 6.7 Hz, 2C), 152.1 (t, $J$ = 2.7 Hz), 148.8 (2C), 140.7 (t, $J$ = 1.7 Hz), 136.4, 134.2, 134.1, 134.0 (t, $J$ = 8.7 Hz, 4C), 133.8, 133.7, 133.5 (t, $J$ = 1.6 Hz), 133.1 (t, $J$ = 8.0 Hz, 4C), 132.4 (2C), 131.0 (2C), 129.0 (2C), 128.9 (4C), 128.7 (2C), 128.3 (t, $J$ = 4.7 Hz, 4C), 128.2 (t, $J$ = 4.5 Hz, 4C), 125.4 (2C), 124.2 (t, $J$ = 2.2 Hz, 2C), 122.3 (t, $J$ = 10.9 Hz), 120.9 (2C), 116.5, 111.2, 36.0 (t, $J$ = 1.5 Hz), 28.9, 27.0, 20.7. MS (FAB, 3-NBA), m/z (%): 678.09 (11), 677.09 (5), 676.08 (12), 657.12 (6), 645.12 (5), 644.12 (22), 643.12 (55), 642.11 (47), 641.11 (100) $[Cu(Xantphos)]^+$, 627.09 (7), 626.09 (8), 625.08 (8), 307.05 (8) [3-NBA], 191.92 (12), 185.01 (6), 184.00 (6), 182.97 (6), 154.97 (8) [3-NBA], 153.96 (29), 137.97 (10), 136.96 (17), 135.95 (19), 106.94 (5) [3-NBA], 88.90 (5). IR (ATR, ν̃) = 3055 (vw), 2964 (vw), 1556 (s), 1509 (w), 1479 (w), 1461 (w), 1432 (s), 1402 (m), 1382 (m), 1292 (s), 1266 (w), 1257 (w), 1239 (vw), 1221 (m), 1208 (w), 1194 (w), 1182 (w), 1170 (w), 1154 (w), 1107 (w), 1093 (w), 1068 (w), 1028 (vs), 997 (vw), 971 (w), 890 (vw), 880 (w), 873 (w), 848 (vw), 825 (w), 814 (w), 798 (w), 778 (w), 745 (s), 731 (vs), 692 (vs), 680 (w), 608 (w), 533 (w), 520 (w), 507 (vs), 495 (m), 488 (m), 478 (w), 458 (m), 447 (w), 424 (m), 418 (w), 412 (w), 404 (w), 401 (w) $cm^{-1}$. EA ($C_{51}H_{45}CuN_2OP_2$): Calcd C, 74.03; H, 5.48; N, 3.39. Found C, 70.81; H, 4.81; N, 3.35.

*Characterization of [Cu($L^2$)($PPh_3$)$_2$]*. Yield: 72% (0.301 g). m.p. > 300 °C. $^1H$ NMR (400 MHz, Chloroform-*d* [7.27 ppm], ppm) δ = 8.17 (s, 1H, $L^2$), 7.30–7.26 (m, 6H, $PPh_3$), 7.23 (d, $J$ = 8.2 Hz, 2H, $L^2$), 7.15–7.13 (m, 25H, $L^2$ + $PPh_3$), 6.99 (d, $J$ = 3.5 Hz, 1H, $L^2$), 6.79 (d, $J$ = 8.3 Hz, 2H, $L^2$), 6.38 (d, $J$ = 3.5 Hz, 1H, $L^2$). $^{31}P\{^1H\}$ NMR (162 MHz, ppm) δ = −1.13. $^{13}C$ NMR (100 MHz, Chloroform-*d* [77.0 ppm], ppm) δ = 155.0, 153.9, 140.8, 138.7, 134.4 (d, $J$ = 23.7 Hz, 6C), 133.7 (d, $J$ = 14.9 Hz, 12C), 129.4 (6C), 128.4 (d, $J$ = 8.3 Hz, 12C), 125.9 (q, $J$ = 3.6 Hz, 2C), 121.8 (2C), 119.1, 113.0. $^{19}F$ NMR (376 MHz, ppm) δ = −61.61. MS (FAB, 3-NBA), m/z (%): 603.13 (9), 590.14 (19), 589.13 (52), 588.14 (42), 587.14 (100) $[Cu(PPh_3)_2]^+$, 564.10 (8), 563.11 (9), 562.10 (12), 327.02 (16), 326.01 (8), 325.02 (40) $[Cu(PPh_3)]^+$, 307.09 (20) [3-NBA], 289.07 (10), 263.08 (8), 262.07 (18), 239.05 (7), 238.05 (5), 185.01 (5), 182.99 (14), 155.03 (16), 154.02 (54) [3-NBA], 152.03 (5), 139.03 (7), 138.03 (18), 137.02 (32) [3-NBA], 136.01 (35), 120.02 (5), 107.02 (11), 91.01 (7), 90.00 (6), 88.98 (10). IR (ATR, ν̃) = 3057 (w), 3043 (w), 3031 (w), 1664 (w), 1587 (w), 1557 (vs), 1513 (s), 1479 (m), 1434 (s), 1415 (w), 1385 (m), 1326 (s), 1309 (w), 1298 (s), 1285 (vs), 1271 (vs), 1231 (w), 1188 (w), 1173 (s), 1153 (s), 1111 (vs), 1094 (vs), 1074 (m), 1064 (vs), 1037 (vs), 1000 (m), 992 (m), 975 (s), 955 (m), 922 (w), 890 (w), 880 (m), 841 (s), 819 (w), 812 (w), 790 (w), 741 (vs), 693 (vs), 637 (w), 619 (w), 609 (m), 595 (w), 527 (w), 506 (vs), 493 (vs), 443 (w) $cm^{-1}$. EA ($C_{48}H_{40}CuF_3N_2P_2$): Calcd C, 69.68; H, 4.87; N, 3.39. Found C, 69.62; H, 4.49; N, 3.35.

*Characterization of [Cu($L^2$)(DPEphos)]*. Yield: 86% (0.365 g). m.p. > 300 °C. $^1H$ NMR (400 MHz, Chloroform-*d* [7.27 ppm], ppm) δ = 8.17 (s, 1H, $L^2$), 7.23–7.07 (m, 24H, $L^2$ + DPEphos), 6.91–6.83 (m, 8H, $L^2$ + DPEphos), 6.70 (dtd, $J$ = 1.7 Hz, $J$ = 3.6 Hz, $J$ = 7.5 Hz, 2H, DPEphos), 6.28 (dd, $J$ = 1.3 Hz, $J$ = 3.5 Hz, 1H, $L^2$). $^{31}P\{^1H\}$ NMR (162 MHz, ppm) δ = −14.16. $^{13}C$ NMR (100 MHz, Chloroform-*d* [77.0 ppm], ppm) δ = 158.6 (t, $J$ = 6.4 Hz, 2C), 154.4, 153.0, 140.8, 138.5 (2C), 134.4 (2C), 133.9 (br, 8C), 132.9 (t, $J$ = 14.7 Hz, 4C), 130.9 (4C), 129.4 (4C), 128.2 (t, $J$ = 4.7 Hz, 6C), 126.2 (t, $J$ = 11.6 Hz, 2C), 125.6 (q, $J$ = 3.6 Hz, 2C), 121.6 (2C), 120.2 (2C), 118.4 (2C), 112.6. $^{19}F$ NMR (376 MHz, ppm) δ = −61.67. MS (FAB, 3-NBA), m/z (%): 840.23 (3), 839.23 (3), 838.22 (4), 617.07 (3), 605.08 (4), 604.08 (19), 603.07 (53), 602.08 (40), 601.07 (100) $[Cu(DPEphos)]^+$, 600.07 (2), 599.07 (2), 353.09 (5), 338.99 (2), 277.04 (2), 198.98 (8), 182.98 (6). IR (ATR, ν̃) = 3055 (w), 1554 (vs), 1514 (m), 1479 (w), 1462 (w), 1434 (vs), 1419 (w), 1383 (m), 1324 (s), 1300 (m), 1282 (vs), 1259 (vs), 1224 (s), 1211 (s), 1171 (vs), 1150 (vs), 1108 (vs), 1096 (vs), 1064 (vs), 1028 (vs), 999 (m), 972 (m), 949 (w), 875 (m), 858 (w), 841 (s), 803 (w), 789 (w), 762 (w), 747 (vs), 737 (vs), 693 (vs), 637 (w), 619 (w), 608 (w), 595 (w), 543 (w), 520 (w), 506 (vs), 484 (s), 476 (s), 436 (w), 414 (s), 395 (w) $cm^{-1}$. EA ($C_{48}H_{38}CuF_3N_2OP_2$): Calcd C, 68.53; H, 4.55; N 3.33. Found C 68.52; H 4.12; N 3.37.

*Characterization of [Cu($L^2$)(Xantphos)]*. Yield: 70% (0.311 g). m.p. > 300 °C. $^1H$ NMR (400 MHz, Chloroform-*d* [7.27 ppm], ppm) δ = 8.27 (s, 1H, $L^2$), 7.50 (dd, $J$ = 1.4 Hz, $J$ = 7.8 Hz, 2H, Xantphos), 7.24 (t, $J$ = 7.2 Hz, 2H, $L^2$), 7.19–7.05 (m, 18H, $L^2$ + Xantphos), 7.02–6.98 (m, 3H, $L^2$ + Xantphos), 6.93–6.89 (m, 3H, $L^2$), 6.58 (d, $J$ = 8.2 Hz, 2H, Xantphos), 6.44–6.40 (m, 2H, Xantphos), 6.29 (dd, $J$ = 1.2 Hz, $J$ = 3.5 Hz, 1H, $L^2$), 1.83 (s, 3H, Xantphos), 1.64 (s, 3H, Xantphos). $^{31}P\{^1H\}$ NMR (162 MHz, ppm) δ = −13.93. $^{13}C$ NMR (100 MHz, Chloroform-*d* [77.0 ppm], ppm) δ = 155.4 (t, $J$ = 6.5 Hz, 2C), 154.4, 152.9 (t, $J$ = 2.7 Hz), 140.7 (t, $J$ = 1.8 Hz, 2C), 138.3 (2C), 134.2 (t, $J$ = 8.7 Hz, 2C), 133.9 (t, $J$ = 14.3 Hz), 133.6 (t, $J$ = 1.3 Hz), 133.4 (t, $J$ = 16.2 Hz), 132.6 (t, $J$ = 7.9 Hz, 2C), 130.9, 129.4, 128.7 (2C), 128.3 (t, $J$ = 4.8 Hz, 8C), 128.1 (t, $J$ = 4.6 Hz, 8C), 125.6, 125.4 (q, $J$ = 3.8 Hz, 2C), 124.4 (t, $J$ = 1.9 Hz, 2C), 122.0 (t, $J$ = 11.1 Hz, 2C), 120.9, 118.5, 112.5, 36.1 (t, $J$ = 1.4 Hz), 29.7, 25.7. $^{19}F$ NMR (376 MHz, ppm) δ = −61.63. MS (FAB, 3-NBA), m/z (%): 657.16 (6), 645.15 (5), 644.15 (22), 643.15 (54), 642.15 (46), 641.14 (100) $[Cu(Xantphos)]^+$, 627.12 (6), 626.12 (8), 625.11 (7), 307.08 (5) [3-NBA], 155.02 (5), 154.02 (17) [3-NBA], 138.03 (5), 137.02 (10) [3-NBA], 136.01 (12). IR (ATR, ν̃) = 3064 (vw), 2965 (w), 1551 (vs), 1513 (m), 1479 (w), 1435 (m), 1402 (vs), 1384 (s), 1323 (s), 1307 (w), 1276 (vs), 1222 (vs), 1187 (m), 1169 (vs), 1106 (vs), 1062 (vs), 1031 (vs), 999 (m), 970 (m), 959 (m), 921 (w), 881 (m), 861 (w), 839 (m), 815 (w), 789 (w), 779 (w), 745 (vs), 731 (vs), 693 (vs), 680 (s), 637 (w), 606 (w), 589 (w), 533 (w), 506 (vs), 483 (m), 466 (s), 433 (w), 411 (m), 392 (w), 384 (w) $cm^{-1}$. EA ($C_{51}H_{42}CuF_3N_2OP_2$): Calcd C 69.50; H 4.80; N 3.18. Found C 69.54; H 4.42; N 3.25.

*Characterization of [Cu($L^3$)($PPh_3$)$_2$]*. Yield: 70% (0.296 g). m.p. 169 °C (dec.). $^1H$ NMR (400 MHz, Chloroform-*d* [7.27 ppm], ppm) δ = 8.14 (s, 1H, $L^3$), 7.31 (m, 7H, $L^3$ + $PPh_3$), 7.23–7.15 (m, 25H, $L^3$ + $PPh_3$), 7.10–7.08 (m, 2H, $L^3$), 6.93 (d, $J$ = 3.5 Hz, 1H, $L^3$), 6.65–6.61 (m, 1H, $L^3$), 6.35 (d, $J$ = 4.3 Hz, 1H, $L^3$). $^{31}P\{^1H\}$ NMR (162 MHz, ppm) δ = −1.75. $^{13}C$ NMR (100 MHz, Chloroform-*d* [77.0 ppm], ppm) δ = 153.7, 151.0, 140.7 (6C), 138.0 (2C), 134.2, 133.8 (d, $J$ = 15.2 Hz, 12C), 131.6 (2C), 129.5 (6C), 128.5 (d, $J$ = 8.9 Hz, 12C), 123.4, 118.3, 116.2, 112.5. MS (FAB, 3-NBA), m/z (%): 678.10 (17), 676.09 (17), 603.13 (10), 590.14 (19), 589.14 (53), 588.14 (41), 587.14 (100) $[Cu(PPh_3)_2]^+$, 327.02 (46), 326.02 (19), 325.02 (95) $[Cu(PPh_3)]^+$, 279.07 (18), 277.08 (12), 263.07 (30), 262.07 (79), 247.96 (10), 233.05 (12), 195.08 (10), 185.01 (22), 183.00 (50), 154.02 (30) [3-NBA], 138.03 (10), 137.02 (18) [3-NBA], 136.01 (25), 107.02 (10), 88.99 (13). IR (ATR, ν̃) = 3054 (w), 1589 (w), 1554 (vs), 1500 (w), 1477 (m), 1434 (s), 1401 (w), 1383 (m), 1298 (s), 1275 (m), 1222 (w), 1184 (m), 1170 (m), 1159 (w), 1094 (m), 1069 (w), 1040 (s), 1027 (m), 999 (w), 976 (w), 956 (w), 891 (w), 877 (w), 827 (w), 806 (w), 778 (w), 739 (vs), 691 (vs), 642 (w), 632 (w), 619 (w), 609 (w), 527 (w), 504 (vs), 490 (vs), 443 (w), 416 (w), 402 (w) $cm^{-1}$. EA ($C_{47}H_{40}BrCuN_2P_2$): Calcd C 67.34; H 4.81; N 3.34. Found C 67.10; H 4.54; N 2.68.

*Characterization of [Cu($L^3$)(DPEphos)]*. Yield: 71% (0.274 g). m.p. 198 °C (dec.). $^1H$ NMR (400 MHz, Chloroform-*d* [7.27 ppm], ppm) δ = 8.13 (s, 1H, $L^3$), 7.23–7.10 (m, 22H, $L^3$ + DPEphos), 6.98–6.94 (m, 2H, $L^3$ + DPEphos), 6.91–6.84 (m, 4H, DPEphos), 6.79 (d, $J$ = 3.5 Hz, 1H, $L^3$), 6.75–6.69 (m, 4H, $L^3$ + DPEphos), 6.27 (d, $J$ = 4.0 Hz, 1H, $L^3$). $^{31}P\{^1H\}$ NMR (162 MHz, ppm) δ = −15.01. $^{13}C$ NMR (100 MHz, Chloroform-*d* [77.0 ppm], ppm) δ = 158.6 (t, $J$ = 6.5 Hz, 2C), 152.7 (t, $J$ = 2.7 Hz), 150.5, 140.7 (t, $J$ = 1.5 Hz), 137.8, 134.4 (2C), 133.9–133.7 (m, 8C), 133.0 (t, $J$ = 15.0 Hz, 4C), 131.2 (2C), 130.8 (4C), 129.2 (2C), 128.2 (t, $J$ = 4.8 Hz, 8C), 126.3 (t, $J$ = 11.4 Hz, 2C), 124.3 (t, $J$ = 1.7 Hz, 2C), 123.3 (2C), 120.2 (t, $J$ = 1.8 Hz, 2C), 117.5 (t, $J$ = 1.7 Hz), 115.8, 112.1.

Research Article
doi.org/10.1002/ejic.202400080



MS (FAB, 3-NBA), m/z (%): 657.12 (8), 645.11 (5), 644.12 (22), 643.11 (54), 642.11 (45), 641.11 (100) [Cu(DPEphos)]$^+$, 628.08 (5), 627.08 (7), 626.08 (9), 625.08 (8), 154.02 (9) [3-NBA], 137.02 (6) [3-NBA], 136.02 (7). IR (ATR, $\tilde{\nu}$) = 3060 (vw), 1587 (w), 1557 (vs), 1503 (w), 1470 (m), 1458 (w), 1432 (vs), 1397 (w), 1383 (s), 1290 (vs), 1258 (w), 1213 (vs), 1186 (m), 1157 (w), 1125 (w), 1094 (w), 1068 (w), 1031 (vs), 1006 (w), 975 (w), 945 (w), 878 (m), 863 (w), 834 (w), 807 (w), 800 (w), 778 (w), 738 (vs), 693 (vs), 612 (w), 545 (m), 523 (m), 509 (s), 496 (s), 489 (s), 475 (s), 445 (w), 435 (w), 422 (w), 411 (w) cm$^{-1}$. EA ($C_{47}H_{38}BrCuN_2OP_2$): Calcd C 66.24; H 4.49; N 3.29. Found C 65.88; H 4.17; N 3.41.

*Characterization of [Cu(L$^3$)(Xantphos)].* Yield: 81% (0.363 g). m.p. 237 °C (dec.). $^1$H NMR (400 MHz, Chloroform-*d* [7.26 ppm], ppm) δ = 8.32 (s, 1H, L$^3$), 7.61 (dd, *J* = 7.8 Hz, *J* = 1.4 Hz, 2H, Xantphos), 7.32 (t, *J* = 7.3 Hz, 2H, L$^3$), 7.20 (m, 18H, L$^3$ + Xantphos), 7.09 (t, *J* = 7.7 Hz, 2H, Xantphos), 7.01 (d, *J* = 3.5 Hz, 1H, L$^3$), 6.92 (s, 1H, L$^3$), 6.88–6.86 (m, 2H, Xantphos), 6.56–6.51 (m, 4H, L$^3$ + Xantphos), 6.35–6.34 (m, 1H, L$^3$), 1.91 (s, 3H, Xantphos), 1.73 (s, 3H, Xantphos). $^{31}$P{$^1$H} NMR (162 MHz, ppm) δ = −14.10. $^{13}$C NMR (100 MHz, Chloroform-*d* [77.0 ppm], ppm) δ = 155.4 (t, *J* = 6.5 Hz, 2 C), 152.4 (t, *J* = 2.7 Hz), 150.4, 140.6 (t, *J* = 1.7 Hz, 2C), 137.5, 134.1 (t, *J* = 8.3 Hz, 4C), 134.1, 133.9, 133.8, 133.7 (t, *J* = 15.5 Hz, 2C), 133.6 (t, *J* = 1.4 Hz, 2C), 132.8 (t, *J* = 8.0 Hz, 4C), 131.2 (2C), 130.9, 129.3 (2C), 128.7 (2C), 128.3 (t, *J* = 4.7 Hz, 4C), 128.1 (t, *J* = 4.6 Hz, 4C), 125.6 (2C), 124.4, 122.6 (2C), 122.1 (t, *J* = 11.0 Hz), 117.7 (t, *J* = 1.6 Hz), 115.4, 112.1, 36.1 (t, *J* = 1.5 Hz), 29.5, 26.2. MS (FAB, 3-NBA), m/z (%): 657.12 (8), 645.11 (5), 644.12 (22), 643.11 (54), 642.11 (45), 641.11 (100) [Cu(Xantphos)]$^+$, 628.08 (5), 627.08 (7), 626.08 (9), 625.08 (8), 154.02 (9) [3-NBA], 137.02 (6), 136.02 (7) [3-NBA]. IR (ATR, $\tilde{\nu}$) = 3051 (vw), 2962 (w), 2921 (vw), 1587 (w), 1550 (vs), 1496 (w), 1470 (m), 1434 (s), 1401 (vs), 1381 (s), 1363 (w), 1283 (vs), 1239 (w), 1222 (vs), 1181 (s), 1167 (m), 1152 (w), 1119 (w), 1095 (m), 1068 (w), 1028 (vs), 1001 (m), 970 (m), 950 (w), 875 (m), 824 (m), 792 (w), 788 (w), 776 (m), 752 (s), 737 (vs), 691 (vs), 642 (w), 618 (w), 608 (w), 586 (w), 534 (m), 509 (vs), 501 (vs), 483 (s), 467 (s), 435 (w), 411 (w), 398 (w) cm$^{-1}$. EA ($C_{50}H_{42}BrCuN_2OP_2$): Calcd C 67.30; H 4.74; N 3.14. Found C 67.11; H 4.45; N 3.09.

*Characterization of [Cu(L$^4$)(PPh$_3$)$_2$].* Yield: 85% (0.346 g). m.p. 100 °C (dec.). $^1$H NMR (400 MHz, Chloroform-*d* [7.27 ppm], ppm) δ = 8.17 (s, 1H, L$^4$), 7.30–7.25 (m, 6H, PPh$_3$), 7.16–7.14 (m, 24H, PPh$_3$), 7.07 (s, 1H, L$^4$), 7.00–6.94 (m, 2H, L$^4$), 6.91 (d, *J* = 3.4 Hz, 1H, L$^4$), 6.76–6.70 (m, 2H, L$^4$), 6.34 (dd, *J* = 1.4 Hz, *J* = 3.5 Hz, 1H, L$^4$), 2.43 (s, 3H, L$^4$). $^{31}$P{$^1$H} NMR (162 MHz, ppm) δ −1.41. $^{13}$C NMR (100 MHz, Chloroform-*d* [77.0 ppm], ppm) δ = 153.5, 149.5, 140.6, 137.4, 134.5 (d, *J* = 24.5 Hz, 6C), 133.8 (d, *J* = 15.4 Hz, 12C), 129.3 (6C), 128.4 (d, *J* = 8.1 Hz, 12C), 128.3 (2C), 122.2 (2C), 117.7, 112.1, 17.2. MS (FAB, 3-NBA), m/z (%): 590.10 (20), 589.09 (57), 588.10 (42), 587.10 (100) [Cu(PPh$_3$)$_2$]$^+$, 543.07 (11), 542.08 (25), 541.08 (25), 540.08 (43), 327.00 (48), 326.00 (21), 325.00 (98) [Cu(PPh$_3$)]$^+$, 279.05 (14), 277.97 (11), 277.07 (12), 263.06 (30), 262.05 (67) [PPh$_3$], 233.04 (19), 185.00 (21), 182.99 (48), 154.01 (29) [3-NBA], 137.01 (17), 136.01 (22) [3-NBA]. IR (ATR, $\tilde{\nu}$) = 3053 (vw), 2918 (vw), 1594 (w), 1555 (s), 1500 (w), 1476 (m), 1434 (s), 1402 (w), 1384 (m), 1293 (s), 1273 (m), 1222 (w), 1183 (w), 1171 (w), 1157 (w), 1120 (vw), 1092 (m), 1071 (w), 1035 (s), 996 (w), 973 (w), 958 (w), 891 (w), 878 (w), 851 (vw), 829 (w), 781 (w), 741 (vs), 693 (vs), 618 (w), 611 (w), 547 (vw), 527 (w), 504 (vs), 492 (vs), 452 (w), 441 (w), 428 (w), 416 (w), 382 (w) cm$^{-1}$. EA ($C_{48}H_{43}CuN_2P_2S$): Calcd C 71.58; H 5.38; N 3.48. Found C 71.01; H 5.08; N 3.54.

*Characterization of [Cu(L$^4$)(DPEphos)].* Yield: 60% (0.247 g). m.p. 180 °C (dec.). $^1$H NMR (400 MHz, Chloroform-*d* [7.27 ppm], ppm) δ = 8.16 (d, *J* = 0.9 Hz, 1H, L$^4$), 7.22–7.09 (m, 23H, L$^4$ + DPEphos), 6.91–6.82 (m, 8H, L$^4$ + DPEphos), 6.77 (d, *J* = 3.4 Hz, 1H, L$^4$), 6.74–6.68 (m, 2H, DPEphos), 6.26 (dd, *J* = 1.4 Hz, *J* = 3.5 Hz, 1H, L$^4$), 2.37 (s, 3H, L$^4$). $^{31}$P{$^1$H} NMR (162 MHz, ppm) δ = −15.06. $^{13}$C NMR (100 MHz, Chloroform-*d* [77.0 ppm], ppm) δ = 158.6 (t, *J* = 6.5 Hz, 2C), 152.3 (t, *J* = 2.7 Hz), 149.5, 140.6, 137.3, 134.3 (2C), 133.8 (br, 6C), 133.1 (t, *J* = 15.0 Hz, 4C), 131.3, 130.6 (4C), 129.0 (4C), 128.4 (2C), 128.1 (t, *J* = 4.4 Hz, 8C), 126.3 (t, *J* = 11.4 Hz, 2C), 124.1 (t, *J* = 1.4 Hz, 2C), 122.2 (2C), 120.0 (2C), 116.8, 111.6, 17.5. MS (FAB, 3-NBA), m/z (%): 619.06 (7), 618.07 (5), 617.06 (13), 604.07 (19), 603.07 (52), 602.06 (41), 601.06 (100) [Cu(DPEphos)]$^+$, 353.09 (11), 307.06 (6) [3-NBA], 277.05 (7), 233.03 (7), 217.03 (7), 216.02 (8) [L], 198.98 (14), 182.98 (11), 155.02 (6), 154.01 (22) [3-NBA], 138.02 (7), 137.01 (14), 136.00 (16) [3-NBA], 107.01 (5), 88.98 (5). IR (ATR, $\tilde{\nu}$) = 3063 (w), 3054 (w), 1587 (w), 1562 (vs), 1504 (w), 1476 (m), 1459 (m), 1434 (vs), 1398 (w), 1384 (m), 1290 (vs), 1268 (w), 1258 (m), 1218 (vs), 1187 (m), 1159 (w), 1123 (w), 1092 (m), 1069 (w), 1033 (vs), 1011 (w), 999 (w), 973 (w), 942 (w), 891 (vw), 878 (m), 858 (w), 849 (vw), 829 (w), 802 (w), 778 (w), 737 (vs), 713 (w), 693 (vs), 667 (w), 612 (w), 545 (m), 523 (m), 507 (vs), 489 (s), 473 (s), 446 (w), 431 (w), 421 (w), 412 (w), 397 (vw) cm$^{-1}$. EA ($C_{48}H_{41}CuN_2OP_2S$): Calcd C, 70.36; H, 5.04; N, 3.42; S, 3.91. Found C, 69.57; H, 4.83; N, 3.42; S, 3.76.

*Characterization of [Cu(L$^4$)(Xantphos)].* Yield: 75% (0.325 g). m.p. 100 °C (dec.).$^1$H NMR (400 MHz, Chloroform-*d* [7.27 ppm], ppm) δ = 8.24 (s, 1H, L$^4$), 7.46 (dd, *J* = 1.4 Hz, *J* = 7.8 Hz, 2H, Xantphos), 7.39–7.34 (m, 1H, L$^4$), 7.16–7.09 (m, 9H, L$^4$ + Xantphos), 7.06–6.99 (m, 11H, L$^4$ + Xantphos), 6.94 (t, *J* = 7.7 Hz, 8H, Xantphos), 6.83 (d, *J* = 3.5 Hz, 1H, L$^4$), 6.72 (s, 1H, L$^4$), 6.63–6.56 (m, 4H, L$^4$ + Xantphos), 6.37 (dtd, *J* = 1.4 Hz, *J* = 3.6 Hz, *J* = 7.3 Hz, 2H, Xantphos), 6.18 (dd, *J* = 1.3 Hz, *J* = 3.5 Hz, 1H, L$^4$), 2.28 (s, 3H, L$^4$), 1.76 (s, 3H, Xantphos), 1.60 (s, 3H, Xantphos). $^{31}$P{$^1$H} NMR (162 MHz, ppm) δ = −14.21. $^{13}$C NMR (100 MHz, Chloroform-d [77.0 ppm], ppm) δ = 155.5 (t, *J* = 6.5 Hz, 2C), 152.0 (*t*, J = 2.8 Hz), 149.2, 140.8 (2C), 137.2, 134.2, 134.2 (t, *J* = 8.5 Hz, 6C), 133.9 (t, *J* = 8.5 Hz), 133.8, 133.7, 133.6, 133.0 (t, *J* = 8.2 Hz, 2C), 131.6, 131.3, 131.1, 129.9 (2C), 129.3 (2C), 128.8, 128.7 (t, *J* = 5.0 Hz, 2C), 128.3 (t, *J* = 4.8 Hz, 6C), 128.1 (t, *J* = 4.6 Hz, 2C), 125.6 (2C), 124.4 (2C), 122.4 (t, *J* = 11.1 Hz), 121.6 (2C), 117.2, 111.8, 36.2 (t, *J* = 1.4 Hz), 29.4, 26.5, 17.3. MS (FAB, 3-NBA), m/z (%): 644.14 (22), 643.13 (54), 642.13 (46), 641.13 (100) [Cu(Xantphos)]$^+$, 626.11 (9), 154.01 (13) [3-NBA], 136.01 (10) [3-NBA]. IR (ATR, $\tilde{\nu}$) = 3058 (w), 3048 (w), 2973 (w), 2962 (w), 2921 (w), 1594 (w), 1550 (vs), 1500 (w), 1477 (m), 1434 (s), 1402 (vs), 1383 (vs), 1358 (w), 1288 (vs), 1224 (vs), 1204 (w), 1183 (s), 1171 (s), 1152 (w), 1120 (w), 1094 (m), 1071 (w), 1031 (vs), 997 (w), 972 (w), 956 (w), 877 (m), 820 (w), 790 (w), 779 (m), 748 (vs), 731 (vs), 693 (vs), 680 (s), 667 (m), 608 (w), 533 (w), 506 (vs), 483 (m), 466 (m), 409 (w) cm$^{-1}$. EA ($C_{51}H_{45}CuN_2OP_2S$): Calcd C 71.27; H 5.28; N 3.26; S 3.73. Found C 69.51; H 4.93; N 3.24; S 3.68.

*Characterization of [Cu(L$^5$)(PPh$_3$)$_2$].* Yield: 75% (0.298 g). m.p. 130 °C (dec.). $^1$H NMR (500 MHz, Chloroform-*d* [7.26 ppm], ppm) δ = 8.62 (s, 1H, L$^5$), 7.70–7.64 (m, 2H, L$^5$), 7.55 (m, 1H, L$^5$), 7.47 (m, 1H, L$^5$), 7.33–7.25 (m, 18H, L$^5$ + PPh$_3$), 7.13 (t, *J* = 7.6 Hz, 14H, L$^5$ + PPh3), 6.41 (d, *J* = 3.8 Hz, 1H, L). $^{31}$P{$^1$H} NMR (162 MHz, ppm) δ = −0.80. $^{13}$C NMR (100 MHz, Chloroform-*d* [77.0 ppm], ppm) δ = 153.3, 152.1, 142.7, 140.6, 134.1 (d, *J* = 25.7 Hz, 6C), 133.8 (d, *J* = 14.5 Hz, 12C), 132.2 (d, *J* = 9.9 Hz), 129.4 (6C), 128.6 (d, *J* = 12.2 Hz), 128.3 (d, *J* = 8.5 Hz, 12C), 125.7, 123.8, 122.8, 121.1, 120.7, 116.5. MS (FAB, 3-NBA), m/z (%): 590.10 (19), 589.10 (48), 588.09 (37), 587.10 (100) [Cu(PPh$_3$)$_2$]$^+$, 554.05 (12), 553.05 (13), 552.06 (24), 551.05 (18), 475.02 (12), 326.98 (39), 325.99 (19), 324.99 (83) [Cu(PPh$_3$)]$^+$, 307.04 (9) [3-NBA], 304.04 (10), 279.05 (14), 263.05 (30), 262.04 (68) [PPh$_3$], 228.00 (10), 185.00 (16), 182.98 (40), 155.01 (11), 154.00 (45) [3-NBA], 152.00 (8), 150.99 (17), 149.98 (9), 138.01 (14), 137.01 (28), 136.00 (33) [3-NBA], 107.01 (10), 88.97 (11). IR (ATR, $\tilde{\nu}$) = 3050 (w), 1567 (s), 1499 (w), 1473 (vs), 1455 (m), 1434 (vs), 1375 (vs), 1339 (w), 1313 (w), 1295 (w), 1261 (vs), 1197 (m), 1177 (w), 1163 (s), 1150 (vs), 1128 (m), 1092 (m), 1064 (w), 1024 (vs), 997 (m), 966 (s), 931 (w), 921 (m), 887 (w), 851 (w), 837 (m), 817 (w), 739 (vs), 720 (s), 691 (vs), 662 (s), 628 (w), 618 (w), 601 (w), 551 (w), 527 (w), 516 (vs), 503 (vs), 486 (s), 433 (w), 415

(w), 384 (w) $cm^{-1}$. EA ($C_{48}H_{40}CuN_3P_2S$): Calcd C 70.62; H 4.94; N 5.15. Found C 69.66; H 4.68; N 5.53.

*Characterization of [Cu(L$^5$)(DPEphos)]*. Yield: 38% (0.160 g). m.p. 120 °C (dec.). $^1$H NMR (500 MHz, Chloroform-*d* [7.26 ppm], ppm) δ = 8.54 (s, 1H, L$^5$), 7.71 (d, *J* = 8.0 Hz, 1H, L$^5$), 7.53–7.41 (m, 2H, DPEphos), 7.37–7.27 (m, 3H, L$^5$ + DPEphos), 7.23–6.98 (m, 22H, L$^5$ + DPEphos), 6.94–6.89 (m, 2H, L$^5$ + DPEphos), 6.86 (t, *J* = 7.5 Hz, 2H, L$^5$ + DPEphos), 6.74–6.68 (m, 2H, DPEphos), 6.18 (d, *J* = 3.8 Hz, 1H, L$^5$). $^{31}$P{$^1$H} NMR (162 MHz, ppm) δ = −14.22. $^{13}$C NMR (100 MHz, Chloroform-*d* [77.0 ppm], ppm) δ = 158.7 (t, *J* = 6.4 Hz, 2C), 152.8 (t, *J* = 2.3 Hz), 152.5, 142.5 (t, *J* = 1.8 Hz), 140.5, 134.4 (2C), 134.3 (t, *J* = 8.3 Hz, 2C), 134.4–133.6 (m), 130.6 (4C), 130.0, 129.1 (6C), 128.7 (t, *J* = 5.0 Hz), 128.0 (t, *J* = 4.6 Hz, 8C), 126.3 (t, *J* = 12.3 Hz, 2C), 125.4 (2C), 124.1 (2C), 123.1, 122.3 (2C), 120.9, 120.3, 120.0 (2C), 116.0. MS (FAB, 3-NBA), m/z (%): 604.07 (19), 603.07 (52), 602.07 (42), 601.06 (100) [Cu(DPEphos)]$^+$, 353.07 (8), 199.00 (14), 183.01 (10). IR (ATR, ν̃) = 3047 (w), 1585 (s), 1562 (m), 1494 (s), 1475 (vs), 1434 (vs), 1375 (s), 1367 (m), 1351 (m), 1295 (s), 1281 (m), 1265 (vs), 1242 (s), 1214 (vs), 1183 (m), 1164 (vs), 1152 (vs), 1122 (m), 1095 (m), 1067 (m), 1033 (vs), 1000 (m), 973 (s), 953 (m), 933 (m), 888 (m), 874 (m), 851 (w), 824 (s), 807 (m), 768 (w), 747 (vs), 737 (vs), 722 (s), 694 (vs), 663 (s), 628 (w), 618 (w), 603 (w), 544 (m), 523 (m), 506 (vs), 480 (s), 466 (m), 433 (w), 412 (m) $cm^{-1}$. EA ($C_{48}H_{36}CuN_3OP_2S$): Calcd C 69.60; H 4.38; N 5.07. Found C 65.82; H 4.04; N 4.69.

*Characterization of [Cu(L$^5$)(Xantphos)]*. Yield: 25% (0.110 g). m.p. 120 °C (dec.). $^1$H NMR (400 MHz, Chloroform-d [7.26 ppm], ppm) δ = 8.91 (s, 1H, L$^5$), 7.49 (dd, *J* = 7.7 Hz, *J* = 1.4 Hz, 2H, Xantphos), 7.26–6.96 (m, 27H, L$^5$ + Xantphos), 6.73 (s, 1H, L$^5$), 6.42 (dt, *J* = 7.5 Hz, *J* = 3.7 Hz, 2H, Xantphos), 6.23 (d, *J* = 3.9 Hz, 1H, L$^5$), 1.76 (s, 3H, Xantphos), 1.71 (s, 3H, Xantphos). $^{31}$P{$^1$H} NMR (162 MHz, ppm) δ = −13.73. $^{13}$C NMR (100 MHz, Chloroform-d [77.0 ppm], ppm) δ = 173.9, 155.6 (t, *J* = 6.6 Hz, 2C), 152.8, 151.3 (t, *J* = 2.3 Hz, 2C), 142.4, 141.1 (2C), 134.0 (t, *J* = 8.3 Hz, 4C), 133.8, 133.5, 133.4, 133.2, 133.2 (t, *J* = 8.1 Hz, 4C), 131.3 (2C), 129.9, 129.2 (d, J = 25.0 Hz, 4C), 128.4 (q, *J* = 4.8 Hz, 4C), 125.8 (2C), 125.7 (2C), 124.4 (t, *J* = 2.0 Hz, 2C), 123.9 (2C), 122.3 (t, *J* = 11.9 Hz, 2C), 122.3, 122.1, 120.8 (2C), 120.4, 116.4, 36.2, 28.9, 27.8. MS (FAB, 3-NBA), m/z (%): 644.14 (21), 643.13 (54), 642.13 (45), 641.13 (100) [Cu(Xantphos)]$^+$, 628.11 (6), 627.10 (8), 626.10 (10), 625.10 (9), 153.96 (8) [3-NBA], 135.95 (6) [3-NBA]. IR (ATR, ν̃) = 3050 (w), 2970 (w), 1565 (s), 1499 (m), 1473 (vs), 1456 (m), 1434 (vs), 1402 (vs), 1375 (vs), 1339 (w), 1293 (m), 1261 (vs), 1241 (vs), 1224 (vs), 1196 (s), 1181 (m), 1162 (vs), 1150 (vs), 1120 (s), 1095 (s), 1064 (m), 1027 (vs), 965 (s), 921 (w), 885 (w), 875 (w), 847 (w), 834 (w), 817 (m), 790 (w), 776 (w), 741 (vs), 721 (s), 691 (vs), 660 (s), 629 (w), 618 (w), 601 (w), 588 (w), 533 (w), 507 (vs), 483 (w), 465 (m), 432 (w) $cm^{-1}$. EA ($C_{51}H_{40}CuN_3OP_2S$): Calcd C 70.53; H 4.64; N 4.55. Found C 69.89; H 4.68; N 4.55.

### Crystal Structure Determination

Single crystal X-ray diffraction data were collected on a STOE STADI VARI diffractometer with monochromated Mo–Kα (λ = 0.71073 Å) or Ga–Kα (λ = 1.34143 Å) radiation at 180 K. Using Olex2,[57] the structures were solved with the SHELXT [58] structure solution program using intrinsic phasing and refined with the SHELXL[59] refinement package using least-squares minimization. Refinement was performed with anisotropic temperature factors for all non-hydrogen atoms; hydrogen atoms were calculated on idealized positions. Details regarding the crystal data and structural refinement are given in Tables S1, S3, S5 and S7. Selected bond lengths and angles are collected in Tables S2, S4, S6 and S8.

Deposition Numbers https://www.ccdc.cam.ac.uk/services/structures?id=doi:10.1002/ejic.2024000802308161–2308172 contain the supplementary crystallographic data for this paper. These data are provided free of charge by the joint Cambridge Crystallographic Data Centre and Fachinformationszentrum Karlsruhe https://www.ccdc.cam.ac.uk/structures/ Access Structures service.

### Photoluminescent Measurements

The absorption spectra were collected in dichloromethane solutions employing an Analytik Jena Specord 50 instrument. Room temperature photoluminescence emission (PL) and excitation (PLE) spectra were collected on powder samples using a Horiba Fluorolog-3C-22 spectrofluorometer equipped with a 450 W Xenon lamp. Suitable long-pass filters were placed in front of the acquisition systems to avoid second-order effects. Photoluminescent lifetimes τ were recorded employing multi-channel scaling modality (MCS) triggering the Xe lamp. Photoluminescence quantum yield Φ was measured on solid samples using a Horiba Quanta Phi integrating sphere.

### Cyclic Voltammetry

Cyclic voltammetry experiments were performed with a Gamry Interface 1010B in a three-electrode electrochemical cell. The electrochemical cell was equipped with a glassy carbon disc working electrode, an Ag reference electrode, and a Pt wire as the auxiliary electrode. All the experiments were performed in dry DMF ($5 \cdot 10^{-3}$ M sample, 0.1 M $TBAPF_6$) solution under Ar atmosphere. Ferrocene (Fc) was added after each experiment as an internal standard, according to IUPAC recommendations. The redox properties are reported versus the $Fc/Fc^+$ couple.

### Computational Calculations

The ground-state geometry optimizations were carried out using the global-hybrid *meta*-NGA functional MN15 DFT functional and the Ahlrichs and Weigend's def2 split-valence polarized (def2-SVP) basis set.[60–61] The *C*-PCM implicit solvation model was added to MN15 calculations, considering dichloromethane as continuous medium.[62–63] Excited states and their relative energies were investigated employing TD-DFT (time-dependent DFT) calculations at the same theoretical level, starting from singlet and triplet state optimized geometries.[64] The software used was Gaussian 16 and the output files were elaborated to obtain the hole and electron distributions with the software MultiWFN, version 3.8.[65–66] Cartesian coordinates of the DFT-optimized structures are provided in Table S13.

## Data Deposition in Repositories

The details on the chemical synthesis and original analytical data were added to the repository Chemotion (www.chemotion.net/home).[52]

## *Acknowledgements*

This research has been funded by the Deutsche Forschungsgemeinschaft (DFG, German Research Foundation) under Germany's Excellence Strategy *via* the Excellence Cluster "3D Matter Made to Order" (3DMM2O, EXC-2082/1–390761711, Thrust A1). The authors acknowledge support by the state of Baden-Württemberg through bwHPC and the German Research

Foundation (DFG) through grant no INST 40/575-1 FUGG (JUSTUS 2 cluster), and IFG (KIT) for the access to the Horiba instrument. Open Access funding enabled and organized by Projekt DEAL.

## Conflict of Interests

The authors declare no conflict of interest.

## Data Availability Statement

The data that support the findings of this study are openly available in Chemotion at https://dx.doi.org/10.14272/collection/VF_2023-11-24, reference number 52.

**Keywords:** Schiff base · pyrrole · luminescence · Cu(I) complexes · phosphine

[1] J. Beaudelot, S. Oger, S. Perusko, T. A. Phan, T. Teunens, C. Moucheron, G. Evano, *Chem. Rev.* **2022**, *122*, 16365.
[2] D. Volz, M. Wallesch, C. Fléchon, M. Danz, A. Verma, J. M. Navarro, D. M. Zink, S. Bräse, T. Baumann, *Green Chem.* **2015**, *17*, 1988.
[3] C. Förster, K. Heinze, *Chem. Soc. Rev.* **2020**, *49*, 1057.
[4] X. Hei, S. J. Teat, M. Li, M. Bonite, J. Li, *Inorg. Chem.* **2023**, *62*, 3660.
[5] C. Lecourt, R. Utrera Melero, J. Schiller, F. Moutier, V. Dorcet, G. Calvez, C. Poidevin, K. Costuas, M. Scheer, C. Lescop, *Inorg. Chem. Front.* **2023**, *10*, 6976.
[6] C. Bizzarri, E. Spuling, D. M. Knoll, D. Volz, S. Bräse, *Coord. Chem. Rev.* **2018**, *373*, 49.
[7] R. D. Costa, E. Ortí, H. J. Bolink, F. Monti, G. Accorsi, N. Armaroli, *Angew. Chem. Int. Ed.* **2012**, *51*, 8178.
[8] M. Freitag, J. Teuscher, Y. Saygili, X. Zhang, F. Giordano, P. Liska, J. Hua, S. M. Zakeeruddin, J.-E. Moser, M. Grätzel, A. Hagfeldt, *Nat. Photonics* **2017**, *11*, 372.
[9] V. Ferraro, C. R. Adam, A. Vranic, S. Bräse, *Adv. Funct. Mater.* **2023**, 2302157.
[10] C. Bizzarri, *Eur. J. Org. Chem.* **2022**, *2022*, e202200185.
[11] B. M. Hockin, C. Li, N. Robertson, E. Zysman-Colman, *Catal. Sci. Technol.* **2019**, *9*, 889.
[12] T. P. Nicholls, A. C. Bissember, *Tetrahedron Lett.* **2019**, *60*, 150883.
[13] P. A. Forero Cortés, M. Marx, M. Trose, M. Beller, *Chem. Cat.* **2021**, *1*, 298.
[14] O. S. Wenger, *J. Am. Chem. Soc.* **2018**, *140*, 13522.
[15] C. Wegeberg, O. S. Wenger, *JACS Au* **2021**, *1*, 1860.
[16] Y. Zhang, M. Schulz, M. Wächtler, M. Karnahl, B. Dietzek, *Coord. Chem. Rev.* **2018**, *356*, 127.
[17] Y. Hartmut, *Highly Efficient OLEDs: Materials Based on Thermally Activated Delayed Fluorescence*, Wiley-VHC, Weinheim, Germany, **2019**.
[18] C. Bizzarri, F. Hundemer, J. Busch, S. Bräse, *Polyhedron* **2018**, *140*, 51.
[19] A. Yu Baranov, M. I. Rakhmanova, X. Hei, D. G. Samsonenko, D. V. Stass, I. Yu Bagryanskaya, M. R. Ryzhikov, V. P. Fedin, J. Li, A. V. Artem′ev, *Chem. Commun.* **2023**, *59*, 2923.
[20] H. Yersin, R. Czerwieniec, U. Monkowius, R. Ramazanov, R. Valiev, M. Z. Shafikov, W.-M. Kwok, C. Ma, *Coord. Chem. Rev.* **2023**, *478*, 214975.
[21] J. Zhang, L. Xu, W.-Y. Wong, *Coord. Chem. Rev.* **2018**, *355*, 180.
[22] V. Ferraro, L. Genesin, J. Castro, L. Pietrobon, A. Vavasori, M. Bortoluzzi, *J. Organomet. Chem.* **2023**, *993*.
[23] W.-H. Sun, K. Wang, K. Wedeking, D. Zhang, S. Zhang, J. Cai, Y. Li, *Organometallics* **2007**, *26*, 4781.
[24] K. Wang, K. Wedeking, W. Zuo, D. Zhang, W.-H. Sun, *J. Organomet. Chem.* **2008**, *693*, 1073.
[25] M. Bortoluzzi, G. Paolucci, B. Pitteri, A. Vavasori, *Inorg. Chem. Commun.* **2006**, *9*, 1301.
[26] M. Bortoluzzi, G. Paolucci, B. Pitteri, P. Zennaro, V. Bertolasi, *J. Organomet. Chem.* **2011**, *696*, 2565.
[27] J. Lv, X. Wu, R. Wang, Y. Wu, S. Xu, F. Zhao, Y. Wang, *Polyhedron* **2022**, *224*, 116002.
[28] J. Lv, Q. Li, J. Wang, S. Xu, F. Zhao, H. He, Y. Wang, *J. Mol. Struct.* **2022**, *1252*, 132180.
[29] J. Lv, Y. Lu, J. Wang, F. Zhao, Y. Wang, H. He, Y. Wu, *J. Mol. Struct.* **2022**, *1249*, 131638.
[30] J. M. Busch, D. S. Koshelev, A. A. Vashchenko, O. Fuhr, M. Nieger, V. V. Utochnikova, S. Bräse, *Inorg. Chem.* **2021**, *60*, 2315.
[31] J. M. Busch, D. M. Zink, P. Di Martino-Fumo, F. R. Rehak, P. Boden, S. Steiger, O. Fuhr, M. Nieger, W. Klopper, M. Gerhards, S. Bräse, *Dalton Trans.* **2019**, *48*, 15687.
[32] M. Wallesch, A. Verma, C. Fléchon, H. Flügge, D. M. Zink, S. M. Seifermann, J. M. Navarro, T. Vitova, J. Göttlicher, R. Steininger, L. Weinhardt, M. Zimmer, M. Gerhards, C. Heske, S. Bräse, T. Baumann, D. Volz, *Chem. Eur. J.* **2016**, *22*, 16400.
[33] L. Bergmann, G. J. Hedley, T. Baumann, S. Bräse, I. D. W. Samuel *Sci. Adv.* **2016**, *2*, e1500889.
[34] J. M. Busch, F. R. Rehak, V. Ferraro, M. Nieger, M. Kemell, O. Fuhr, W. Klopper, S. Bräse, *ACS Omega* **2024**, *9*, 2220.
[35] J. Castro, V. Ferraro, M. Bortoluzzi, *New J. Chem.* **2022**, *46*, 18938.
[36] V. Ferraro, J. Castro, L. Agostinis, M. Bortoluzzi, *Transition Met. Chem.* **2021**, *46*, 391.
[37] V. Ferraro, M. Bortoluzzi, J. Castro, A. Vomiero, S. You, *Inorg. Chem. Commun.* **2020**, *116*, 107894.
[38] M. G. Crestani, G. F. Manbeck, W. W. Brennessel, T. M. McCormick, R. Eisenberg, *Inorg. Chem.* **2011**, *50*, 7172.
[39] F. H. Westheimer, K. Taguchi, *J. Org. Chem.* **1971**, *36*, 1570.
[40] A. Kaeser, M. Mohankumar, J. Mohanraj, F. Monti, M. Holler, J.-J. Cid, O. Moudam, I. Nierengarten, L. Karmazin-Brelot, C. Duhayon, B. Delavaux-Nicot, N. Armaroli, J.-F. Nierengarten, *Inorg. Chem.* **2013**, *52*, 12140.
[41] B. Hupp, C. Schiller, C. Lenczyk, M. Stanoppi, K. Edkins, A. Lorbach, A. Steffen, *Inorg. Chem.* **2017**, *56*, 8996.
[42] A. V. Artem′ev, E. P. Doronina, M. I. Rakhmanova, O. A. Tarasova, I. Y. Bagryanskaya, N. A. Nedolya, *Inorg. Chem. Front.* **2019**, *6*, 671.
[43] K. A. Vinogradova, N. A. Shekhovtsov, A. S. Berezin, T. S. Sukhikh, M. I. Rogovoy, A. V. Artem′ev, M. B. Bushuev, *Dalton Trans.* **2021**, *50*, 9317.
[44] I. Nohara, C. Wegeberg, M. Devereux, A. Prescimone, C. E. Housecroft, E. C. Constable, *J. Mater. Chem. C* **2022**, *10*, 3089.
[45] M. R. Son, Y.-J. Cho, H.-J. Son, D. W. Cho, S. O. Kang, *Phys. Chem. Chem. Phys.* **2017**, *19*, 32670.
[46] J. V. C. Edward M. Kober, Richard S. Lumpkin, Thomas J. Meyer, *J. Phys. Chem.* **1986**, *90*, 3722.
[47] R. Englman, J. Jortner, *Mol. Phys.* **1970**, *18*, 145.
[48] V. Ferraro, M. Girotto, J. Castro, M. Bortoluzzi, *Dyes Pigm.* **2023**, *217*, 111388.
[49] L. Bergmann, J. Friedrichs, M. Mydlak, T. Baumann, M. Nieger, S. Bräse, *Chem. Commun.* **2013**, *49*, 6501.
[50] L. Bergmann, C. Braun, M. Nieger, S. Bräse, *Dalton Trans.* **2018**, *47*, 608.
[51] C. Li, C. F. R. Mackenzie, S. A. Said, A. K. Pal, M. A. Haghighatbin, A. Babaei, M. Sessolo, D. B. Cordes, A. M. Z. Slawin, P. C. J. Kamer, H. J. Bolink, C. F. Hogan, E. Zysman-Colman, *Inorg. Chem.* **2021**, *60*, 10323.
[52] V. Ferraro, S. Bräse, Chemotion Repository 2023. https://dx.doi.org/10.14272/collection/VF_2023-11-24.
[53] S. Tabthong, T. Nanok, P. Kongsaeree, S. Prabpai, P. Hormnirun, *Dalton Trans.* **2014**, *43*, 1348.
[54] B.-C. Xu, T. Hu, J.-Q. Wu, N.-H. Hu, Y.-S. Li, *Dalton Trans.* **2009**, 8854.
[55] A. I. Rodrigues, P. Krishnamoorthy, C. S. B. Gomes, N. Carmona, R. E. Di Paolo, P. Pander, J. Pina, J. S. Seixas de Melo, F. B. Dias, M. J. Calhorda, A. L. Maçanita, J. Morgado, P. T. Gomes, *Dalton Trans.* **2020**, *49*, 10185.
[56] S. S. Thakkar, P. Thakor, A. Ray, H. Doshi, V. R. Thakkar, *Bioorg. Med. Chem.* **2017**, *25*, 5396.
[57] O. V. Dolomanov, L. J. Bourhis, R. J. Gildea, J. A. K. Howard, H. Puschmann, *J. Appl. Crystallogr.* **2009**, *42*, 339.
[58] G. M. Sheldrick, *Acta Crystallogr.* **2015**, *A71*, 3.
[59] G. M. Sheldrick, *Acta Crystallogr.* **2015**, *C71*, 3.
[60] H. S. Yu, X. He, S. L. Li, D. G. Truhlar, *Chem. Sci.* **2016**, *7*, 5032.
[61] F. Weigend, R. Ahlrichs, *Phys. Chem. Chem. Phys.* **2005**, *7*, 3297.
[62] M. Cossi, N. Rega, G. Scalmani, V. Barone, *J. Comput. Chem.* **2003**, *24*, 669.
[63] V. Barone, M. Cossi, *J. Phys. Chem. A* **1998**, *102*, 1995.
[64] C. A. Ulrich, *Time-dependent density functional theory*, Oxford University Press, Oxford, **2012**.
[65] Gaussian 16, Revision C.01, M. J. Frisch, G. W. Trucks, H. B. Schlegel, G. E. Scuseria, M. A. Robb, J. R. Cheeseman, G. Scalmani, V. Barone, G. A. Petersson, H. Nakatsuji, X. Li, M. Caricato, A. V. Marenich, J. Bloino, B. G. Janesko, R. Gomperts, B. Mennucci, H. P. Hratchian, J. V. Ortiz, A. F. Izmaylov, J. L. Sonnenberg, D. Williams-Young, F. Ding, F. Lipparini, F.

Research Article
doi.org/10.1002/ejic.202400080



Egidi, J. Goings, B. Peng, A. Petrone, T. Henderson, D. Ranasinghe, V. G. Zakrzewski, J. Gao, N. Rega, G. Zheng, W. Liang, M. Hada, M. Ehara, K. Toyota, R. Fukuda, J. Hasegawa, M. Ishida, T. Nakajima, Y. Honda, O. Kitao, H. Nakai, T. Vreven, K. Throssell, J. A. Montgomery, Jr., J. E. Peralta, F. Ogliaro, M. J. Bearpark, J. J. Heyd, E. N. Brothers, K. N. Kudin, V. N. Staroverov, T. A. Keith, R. Kobayashi, J. Normand, K. Raghavachari, A. P. Rendell, J. C. Burant, S. S. Iyengar, J. Tomasi, M. Cossi, J. M. Millam, M. Klene, C. Adamo, R. Cammi, J. W. Ochterski, R. L. Martin, K. Morokuma, O. Farkas, J. B. Foresman, and D. J. Fox, Gaussian, Inc., Wallingford CT, 2016.

[66] T. Lu, F. Chen, *J. Comput. Chem.* **2012**, *33*, 580.

Manuscript received: February 7, 2024
Revised manuscript received: April 9, 2024
Accepted manuscript online: April 17, 2024
Version of record online: ■■, ■■

# RESEARCH ARTICLE

Neutral heteroleptic Cu(I) complexes with pyrrole-derived Schiff bases as chelating N-donors exhibited noticeable orange-red emission upon excitation with near-UV and blue light. Experimental and computational data indicate that the photoluminescent properties are ascribable to mixed ligand-centered and metal-to-ligand transitions involving triplet-emitting states.

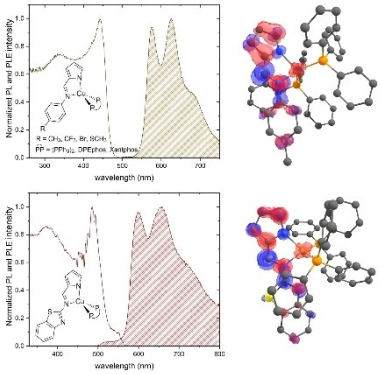


*Dr. V. Ferraro*, Dr. O. Fuhr, Dr. C. Bizzarri, Prof. Dr. S. Bräse**

1 – 12

**Substituted Pyrrole-based Schiff Bases: Effect On The Luminescence Of Neutral Heteroleptic Cu(I) Complexes**